THE ASTROPHYSICAL JOURNAL, 379:L33–L36, 1991 September 20

DISCOVERY OF A FAST RADIATIVE SHOCK WAVE IN THE CYGNUS LOOP USING THE HOPKINS ULTRAVIOLET TELESCOPE

WILLIAM P. BLAIR,[1] KNOX S. LONG,[2] OLAF VANCURA,[1] CHARLES W. BOWERS,[1] ARTHUR F. DAVIDSEN,[1]
W. VAN DYKE DIXON,[1] SAMUEL T. DURRANCE,[1] PAUL D. FELDMAN,[1] HENRY C. FERGUSON,[3]
RICHARD C. HENRY,[1] RANDY A. KIMBLE,[4] GERARD A. KRISS,[1] JEFFREY W. KRUK,[1]
H. WARREN MOOS,[1] AND THEODORE R. GULL[4]

Received 1991 June 3; accepted 1991 July 10

ABSTRACT

We have observed the far-ultraviolet spectrum of a bright radiative filament on the eastern edge of the Cygnus Loop supernova remnant using the Hopkins Ultraviolet Telescope aboard the Astro-1 space shuttle mission in 1990 December. These are the first data to resolve the sub–Lyman-α emission of an interstellar shock wave. We observe strong emission lines of C III λ977, N III λ991, and O VI λλ1032, 1038 and many fainter lines, as well as lines seen above Lyman-α in *IUE* spectra of supernova remnants. Comparison of this spectrum with shock model calculations indicates that the emission at this position in the Cygnus Loop is dominated by a ~ 170 km s^{-1} shock wave, although emission from lower shock velocities may also contribute. Both faster and slower shocks have been identified in the Cygnus Loop, but little attention has been given to the possible presence and importance of fast radiative shocks such as the one reported here. We briefly compare these results to *Voyager* UVS spectra of the Cygnus Loop and discuss the more global implications of these data for the understanding of the Cygnus Loop.

Subject headings: nebulae: individual (Cygnus Loop) — nebulae: supernova remnants — shock waves — ultraviolet: spectra

1. INTRODUCTION

The Cygnus Loop is the prototypical "middle-aged" supernova remnant (SNR). At an assumed distance of 770 pc (see Fesen, Blair, & Kirshner 1982; Hester, Raymond, & Danielson 1986), the $\sim 3° \times 4°$ angular extent of the object corresponds to a linear dimension of $\sim 40 \times 54$ pc. Because of its proximity, well-resolved filamentary structure, and relatively low reddening [$E(B-V) = 0.08$; Fesen et al. 1982], the Cygnus Loop is an object of great importance for the study of shock waves and their interaction with the interstellar medium (ISM). The reader is directed to Blair et al. (1991) and McKee & Draine (1991) for more information.

Observations of SNR shock waves below 1200 Å are of great interest because of the new diagnostics available in this wavelength range. O VI λλ1032, 1038 was seen in absorption when *Copernicus* observed stars behind the Vela SNR (Jenkins, Silk, & Wallerstein 1976). Shemansky, Sandel, & Broadfoot (1979) discuss data from three isolated regions in the Cygnus Loop obtained with the *Voyager 2* UVS in 1978. These observations demonstrated that emission line intensities in the 912–1200 Å spectrum of the Cygnus Loop varied with position, but the ~ 30 Å effective resolution of the *Voyager 2* UVS hindered the line identifications. Recently, Blair et al. (1991) have analyzed a large set of *Voyager 2* UVS observations of the Cygnus Loop, providing the first global maps of the Cygnus Loop in far-UV emission lines. They argued, based on comparison with optical and X-ray data on the remnant, that the emission seen by *Voyager* in the 912–1200 Å region is dominated by C III λ977 and O VI λλ1032, 1038.

In this paper, we describe the first observations to resolve unambiguously the sub-Lyα spectrum of a SNR filament into its individual emission line components. In so doing, we have identified a filament in the Cygnus Loop whose emission is dominated by a fast radiative shock wave with velocity near 170 km s^{-1}. The observations and reductions are discussed in § 2, while in § 3 we discuss the interpretation of these data and their possible ramifications.

2. OBSERVATIONS

The observations were carried out with the Hopkins Ultraviolet Telescope (HUT) as part of the Astro-1 space shuttle mission in 1990 December. HUT consists of a 0.9 m mirror that feeds a prime focus spectrograph with a microchannel plate intensifier and reticon detector. First-order sensitivity covers the region from 850 to 1850 Å at 0.5 Å pixel^{-1} with ~ 3 Å resolution. Details of the spectrograph and telescope can be found in Davidsen et al. (1991). An overview of the Astro Observatory is given by Blair & Gull (1990).

The Cygnus Loop observation discussed here was made on 1990 December 6 at 6:08 UT. A $9'.4 \times 116''$ aperture was placed on the filament as shown in Figure 1 (Plate 1), with the long dimension of the aperture at a position angle of 45°. The projected size of the aperture at the assumed distance of 770 pc is 0.03×0.43 pc. Blind positioning relative to nearby preplanned guide stars was used to center the aperture at $\alpha(1950) = 20^h55^m16^s.0$, $\delta(1950) = 30°54'02''.9$. The total integration was 1902 s, with the first two-thirds of the observation occurring in orbital day. The airglow contamination in the day through the large aperture is substantial, and here we report the spectrum as derived only from the last 638 s of data during the orbital night portion of the observation.

[1] Department of Physics and Astronomy, Johns Hopkins University, Charles & 34th Streets, Baltimore, MD 21218.
[2] Space Telescope Science Institute, 3700 San Martin Drive, Baltimore, MD, 21218.
[3] Institute of Astronomy, University of Cambridge, The Observatories, Madingley Road, Cambridge, CB3 0HA, England.
[4] Laboratory for Astronomy and Solar Physics, Code 681, NASA Goddard Space Flight Center, Greenbelt, MD, 20771.

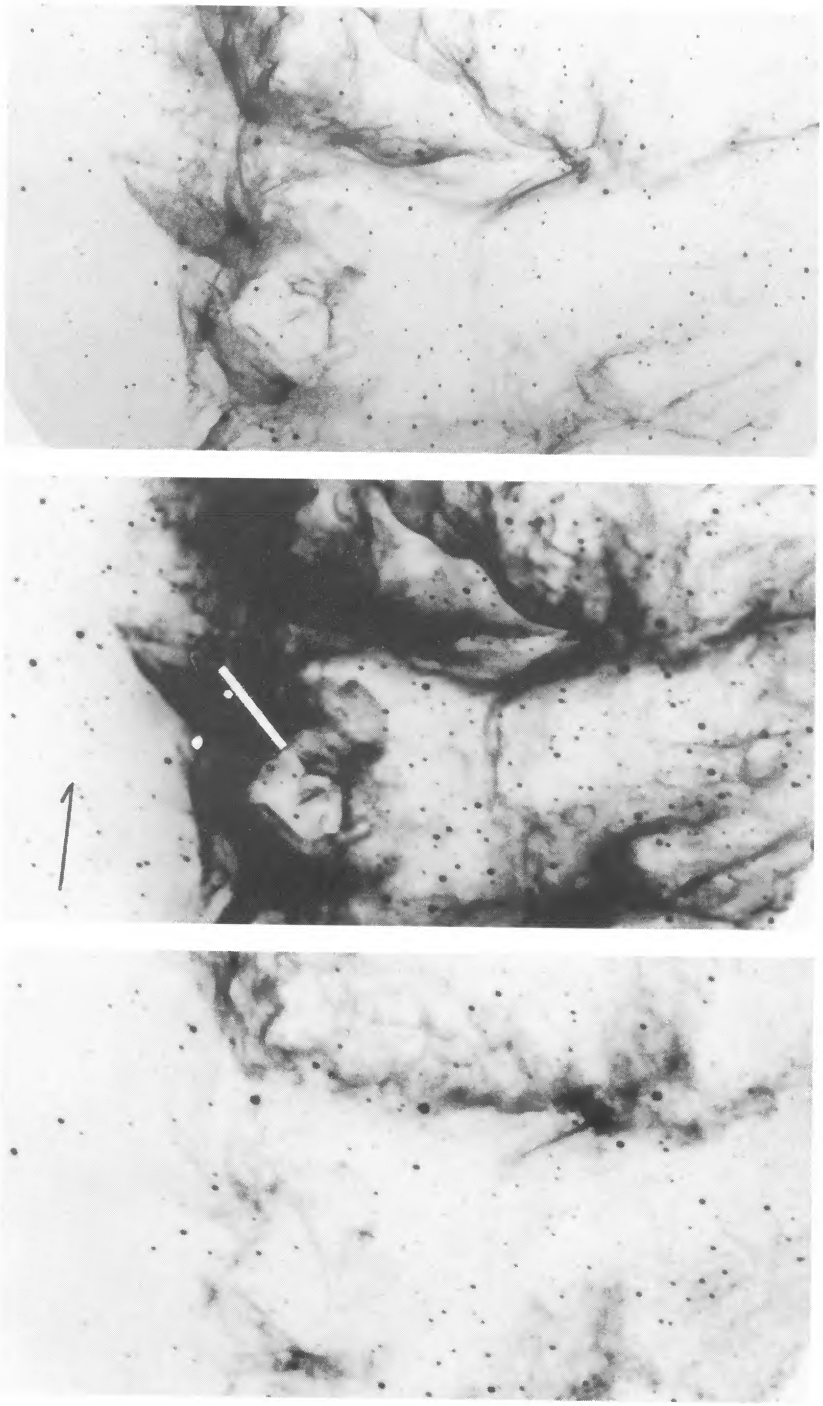

FIG. 1.—Interference filter photographs of the region containing the bright radiative filament observed by HUT. The top two panels are exposures in [O III] λ5007 showing the complex structure and full extent of the filament. The HUT 9.″4 × 116″ aperture is shown to scale in the middle panel and two stars in the overexposed region are indicated for reference. The deeper image shows that the HUT aperture was filled with emission. The bottom panel shows an Hα exposure of the region for comparison. North is indicated by the arrow and east is to the left. Photographs courtesy of Robert Parker.

BLAIR et al. (see 379, L33)

To remove airglow contamination to first-order, we subtracted a comparable portion of a night observation of a blank field. Some residual airglow features remain after this subtraction since the airglow emission is a complicated function of geomagnetic latitude, line-of-sight relative to the Sun and to the Earth limb, and orbital position relative to the terminator. Our flux calibration is based on observations of the white dwarf star G191−B2B compared with model stellar atmospheres as discussed by Davidsen et al. (1991). Line fluxes as measured using the "splot" task of IRAF are shown in Table 1. For well-isolated single lines (including some airglow features), the measured wavelengths appear accurate to within ±0.3 Å and the observed FWHMs are typically in the 3.0 to 3.5 Å range. This is consistent with the slit-limited spectrograph resolution for a diffuse source. The intensities of blended lines from different ions were measured by fitting Gaussians with wavelengths fixed at their laboratory values and forcing the use of a single FWHM. The blend at ~1403 Å includes three O IV] lines and a Si IV line. We have used the fact that the Si IV λ1402.8 line is expected to be half as strong as the 1393.8 Å line to determine total Si IV and O IV] fluxes for comparison with models. Several doublets such as C IV, N V, and O VI are expected to have components in a 2:1 ratio, but C IV and to some extent N V are not well resolved. In this paper we are concerned mainly with the total flux from each doublet for comparison with shock models.

The observed fluxes have been corrected for interstellar reddening by application of an extinction curve derived from Longo et al. (1988). The observed and intrinsic line intensities, scaled relative to C IV(total) = 100, are shown in Table 1. Although the reddening to the Cygnus Loop is not extreme, it causes significant changes in the relative line intensities across the HUT wavelength range because of the steep rise in extinction at the shortest wavelengths. It should be noted that significant variations in UV extinction curves along various lines of sight are known (Mathis 1990, and references therein) and the application of the mean galactic curve has obvious but unavoidable hazards. Uncertainties due to the extinction correction probably dominate over those due to counting statistics for the strong lines in our data. Figure 2 shows the flux-calibrated and reddening-corrected spectrum of the Cygnus Loop radiative filament after smoothing with a 3 pixel boxcar filter. The relative line intensities in this spectrum represent our best estimate of the intrinsic relative line intensities at the observed position.

Many of the emission lines are identified in Figure 2, including the strong transitions of C III λ977, N III λ991, and the well-resolved O VI λλ1032, 1038 doublet. These lines were anticipated in sub-Lyα spectra of SNRs (see Blair et al. 1991) but not clearly resolved with *Voyager*. The presence of O VI emission was confirmed with a rocket experiment by Rasmussen & Martin (1990). The wavelength coverage of HUT also permits the strength of these lines to be compared with those of important lines seen in *IUE* spectra of SNRs, including N V λλ1238, 1242 and C IV λλ1548, 1551. (Indeed, HUT's spectral resolution permits many blends such as N V, O III] λλ1661, 1666, and O IV] + Si IV [~1400 Å] to be resolved at least partially.)

In addition to the new lines seen in the sub-Lyα region, a number of new lines are also detected in the *IUE* range. The O V λ1371, N IV] λ1486, and N III] λ1750 lines have occasionally been seen in SNR spectra, but the latter two in particular are in noisy regions of the SWP camera on *IUE* and are seldom measurable. Newly identified weak features include lines of [Ne IV] λ1602, [Ne V] λλ1146, 1575, and N III] λ1730. Another new feature at 1085 Å is mainly He II; this line could be used with λ1640 to make an independent estimate of the extinction if the conditions in the He^+ zone could be established with confidence (see Osterbrock 1989). However, this line may also include faint emission from N II λ1085.1.

TABLE 1

COMPARISON OF HUT SPECTRUM TO SHOCK MODELS

		OBSERVATIONS[a]		MODELS[b]		
ION	λ (Å)	$F(\lambda)$	$I(\lambda)$[c]	E140	E160	E180
C III	977	42.7	69.2	66.9	61.1	72.8
N III	991	27.8	43.7	9.3	16.2	12.3
Lyβ	1026	<31.	<45.	...	...	...
$O\ VI_{tot}$	1035	136.	198.	0.42	52.5	434.
He II + N II	1085	5.3	7.0	...	...	...
[Ne V]	1146	4.6	5.7	0.26	3.7	8.9
$N\ V_{tot}$	1240	56.2	63.7	5.6	57.4	52.9
C II	1335	8.9	9.5	13.2	17.8	20.6
O V	1371	18.1	19.0	...	...	...
$Si\ IV_{tot}$	1397	20.1	20.9	2.7	5.2	5.9
$O\ IV]_{tot}$	1403	118.	123.	11.3	39.0	42.1
N IV]	1486	27.8	28.1	3.8	8.9	5.4
$C\ IV_{tot}$	1550	100.	100.	100.	100.	100.
[Ne V]	1575	5.9	5.9	0.03	0.3	0.7
[Ne IV]	1602	12.1	12.0	1.0	2.8	3.6
He II	1640	60.2	59.4	4.5	6.5	5.6
$O\ III]_{tot}$	1665	89.8	88.5	10.8	22.9	23.4
N III]	1730	4.3	4.2	...	...	...
$N\ III]_{tot}$	1750	27.5	27.0	3.8	6.4	5.3

[a] Scaled relative to C IV(1550) = 100. $F(1550) = 1.90 \times 10^{-12}$ ergs cm^{-2} s^{-1}; $I(1550) = 3.43 \times 10^{-12}$ ergs cm^{-2} s^{-1}.

[b] Equilibrium pre-ionization models from Hartigan et al. 1987.

[c] Reddening correction assumes $E(B-V) = 0.08$ and the extinction curve of Longo et al. 1988.

3. DISCUSSION

The filament we observed is on the edge of the field studied in detail by Hester, Parker, & Dufour (1983). Optically, the

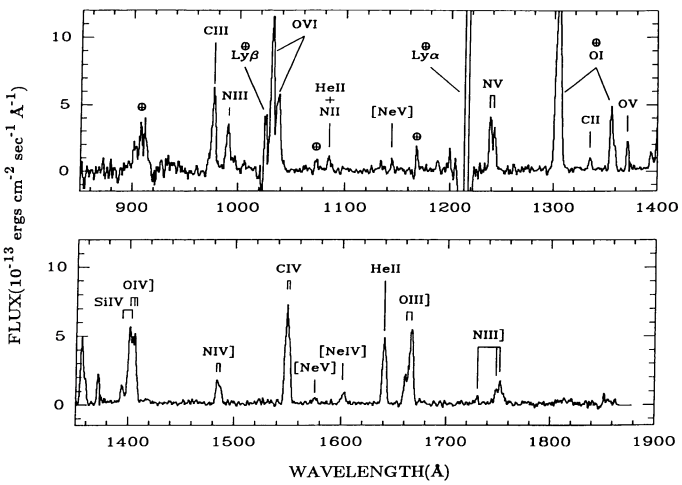

FIG. 2.—Flux-calibrated and reddening-corrected HUT spectrum of the filament indicated in Fig. 1, after smoothing over three pixels. SNR lines are shown in their correct relative intensities. An airglow spectrum from a night observation with HUT has been subtracted, removing Lyα and Lyβ to first order. Remaining air glow features are marked with an Earth symbol. The C III λ977, N III λ991, and O VI λλ1032, 1038 lines (resolved from geocoronal Lyβ and from each other) are seen clearly for the first time.

filament is dominated by emission from [O III] λλ4959, 5007, implying the absence or near absence of the hydrogen recombination zone of the shock. This phenomenon, often called an incomplete or nonsteady flow shock, indicates a relatively recent encounter between the main blast wave and a cloud, so that the shock has not had time to establish a full cooling and recombintion zone. Many such filaments are known in the Cygnus Loop (see Fesen et al. 1982), but this one is bright and well-isolated, which is partly why the filament was chosen for this study.

The optical morphology of the filament is complex (see Fig. 1), with several high surface brightness regions surrounded by lower surface brightness diffuse emission of the same character (Hester et al. 1983). Hence, while the aperture was filled with emission, the illumination was not uniform. Given the variation in filament appearances in optical emission lines (see Fesen et al. 1982), it may be inaccurate to assume that the higher ionization UV emission lines are distributed in the same manner as the optical emission, although one would not expect extreme differences. A comparison of the Ultraviolet Imaging Telescope images (obtained simultaneously with our observation) with optical images of the region will be illuminating in this regard. This filament does not have the appearance of a crisp, edge-on sheet of gas (see Hester 1987), and thus we do not expect resonance line scattering (Raymond et al. 1981) to seriously affect the line intensities.

For comparison with the intrinsic line intensities, we show in Table 1 the line intensities predicted by three steady flow shock models from Hartigan, Raymond, & Harmann (1987, hereafter HRH). The models shown are from the HRH "E" series, which assume equilibrium pre-ionization and preshock densities of 100 cm^{-3}. These densities are higher than expected for the Cygnus Loop, but are not so high as to affect the relative UV line intensities. The models have been scaled in the same manner as the observations. Given the "incompleteness" of the shock as discussed above, one would not expect such models to produce a fit to all lines. However, a comparison for the highest ionization lines should constrain the shock velocity at the observed position since the highest ionization lines are indicative of the peak postshock temperature.

An inspection of Table 1 and Figure 3 demonstrates the power of O VI as a diagnostic for fast shocks. Figure 3 shows the tracking of various ratios from the HRH E models as a function of shock velocity. O VI does not "turn on" in the shock models until about 160 km s^{-1}. The observed O VI/N V and O VI/C IV ratios both predict a shock velocity between 165 and 170 km s^{-1} at the position we have observed. The N V/C IV and C IV/C III ratios are consistent with shock velocities greater than 130 km s^{-1} but provide no other information. An exploratory *IUE* observation (SWP 17666, 105 minutes, unpublished) at nearly the same position as our observation indicated a possible shock velocity near 145 km s^{-1}, based on the (poorly determined) N V/C IV ratio. However, even if an accurate N V/C IV ratio had been obtained by *IUE* it would not have provided an accurate shock velocity at this position because the velocity is too high (i.e., the N V/C IV ratio has "saturated" in terms of its sensitivity to shock velocity below 160 km s^{-1}). Likewise, the C IV/C III ratio is sensitive to shock velocity at lower velocities, but can only be used as a consistency check for the current position.

Under the assumption that the cooling and recombination zone of the shock is complete through the C IV zone, the consistency in the ratios from O VI, N V, and C IV argues for relative abundances of these elements similar to the cosmic abundances assumed in the models. Hence, any carbon depletion onto grains may have been undone by the fast shock. On the other hand, the assumption that the observed filament represents an incomplete shock with velocity near 170 km s^{-1} is not consistent with the strength of the intermediate ionization lines (see Table 1). "Incompleteness" would imply that the intermediate and low ionization lines would be weaker than predicted by the steady flow models since the zone of the shock producing these lines has yet to form. C III λ977 is near the expected intensity from a steady flow 170 km s^{-1} model, but N III λ991, N III] λ1750, O III] λ1665, N IV] λ1486, O IV] λ1403, and Si IV λ1394 are all significantly *stronger* than predicted. This may indicate that lower velocity shocks are also present within the aperture. This would not be surprising given the complex morphology of the filament. If the optical brightness variations are due to changes in density (i.e., cloud/halo morphology), one might expect velocity variations a priori.

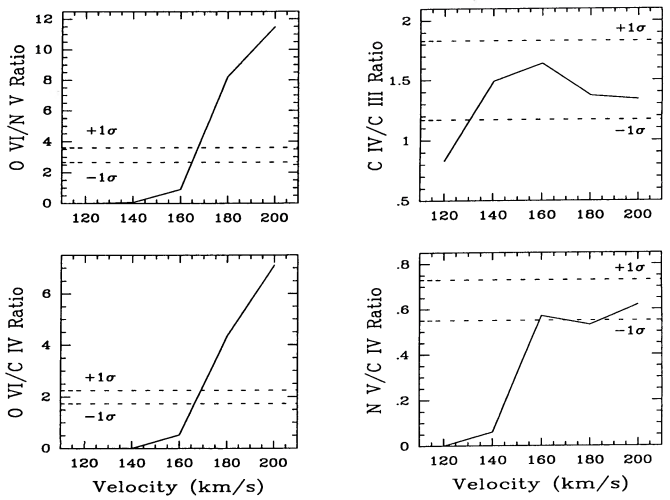

FIG. 3.—Comparison of observed relative line intensities (horizontal dashed lines) with predictions from Hartigan et al. (1987) E series shock models. The range indicated by the dashed lines includes 1 σ errors in the ratio from count statistics only, and does not attempt to quantify errors from reddening uncertainties. The ratios involving O VI indicate a peak shock velocity between 165 and 170 km s^{-1}. Ratios involving lower ionization lines are consistent with this value but cannot be used to discriminate the velocity.

Another possible cause of velocity variations might be instabilities in the postshock flow. Innes, Giddings, & Falle (1987) have calculated dynamical models of radiative shocks and find shocks faster than ~150 km s^{-1} to be unstable in the sense that ionization in the postshock gas simply cannot keep up with the cooling via radiation. Raymond, Wallerstein, & Balick (1991) believe they have found evidence for this effect in the Vela supernova remnant. The effect can cause variations in the velocity of the primary shock involved as well as causing formation of secondary shocks in the flow. To first order, both of these effects might be expected to enhance the line emission in the intermediate ionization lines, as we observe. A detailed accounting of this effect needs to be undertaken, but is beyond the scope of this *Letter*.

The uncertainty in the extent of the completeness of the fast shock makes it difficult to assess the range of shock velocities that might be present. If slower shocks contribute significantly to the N V and C IV line intensities then the peak velocity could be even higher than 170 km s^{-1} (see Fig. 3). This would imply

that the consistent velocity estimated using O VI, N V, and C IV was fortuitous. Shocks in the 120–150 km s^{-1} range produce copious N V and C IV, and may be ruled out by this argument. Shocks with velocities of 100–120 km s^{-1} could produce significant emission in the intermediate ionization lines, although some contribution to C IV would be unavoidable. Even these shocks, if present, would have to be incomplete to prevent such lines as C II λ1335 and the optical Balmer lines from being stronger than observed.

A significant piece of the puzzle is the strength of He II λ1640, which is much stronger relative to C IV than predicted by the steady flow models and cannot be explained by mixing in lower velocity material. *IUE* observations by Raymond et al. (1983) of a faint Balmer-dominated optical filament in the northeast Cygnus Loop also show this signature. In many respects, such filaments represent extreme versions of incomplete shocks, since nearly all of the cooling and recombination zone is missing. Thus the HUT aperture may include emission from both a fast, very incomplete shock (i.e., only complete through the C IV zone) and a slower, incomplete shock. Further work, including high-resolution optical spectroscopy at this position and detailed modeling using truncated (i.e., incomplete) shock models, will be needed to unravel this rather complex situation.

Because fast radiative shocks ($\geq$150 km s^{-1}) have not been identified in the Cygnus Loop previously, we briefly discuss the ramifications of this observation. We clearly confirm the suspected line identifications proposed for the *Voyager* spectral features by Blair et al. (1991); their "1035 Å" map does correspond to the distribution of O VI emission, and the "980 Å" map is dominated by C III λ977 (with some contribution from N III λ991 at positions such as the one reported here). The inescapable conclusion is that O VI emission is widely distributed throughout the Cygnus Loop, even in regions with little optical emission, although the total luminosity is dominated by regions in the east, northeast, and west portions of the remnant, where the optical and X-ray emission are also bright. Nonradiative shocks, perhaps even the primary shock as inferred from the X-ray data, may be responsible for the more distributed component of O VI emission in the Cygnus Loop as well as some of the emission in the east, northeast and west. However, the HUT observation confirms that fast radiative shocks also make a substantial contribution to the O VI luminosity of the Cygnus Loop. Filaments with optical characteristics similar to those of the position we have observed are found throughout the bright optical filamentary structure of the Cygnus Loop (Fesen et al. 1982). Regions of high surface brightness such as the position we have observed may dominate the total O VI luminosity even though the filling factor of this emission may be relatively small.

It is a pleasure to thank the Spacelab Operations Support group at Marshall Space Flight Center for their support during the Astro-1 mission. We also thank the crew of the Astro-1 mission for their efforts to overcome the problems encountered during the flight. Mission Specialist Robert Parker also kindly provided the images used in Figure 1. The Hopkins Ultraviolet Telescope project is supported by NASA contract 5-27000 to Johns Hopkins University.

REFERENCES

Blair, W. P., & Gull, T. R. 1990, Sky & Telescope, 79, 591
Blair, W. P., Long, K. S., Vancura, O., & Holberg, J. B. 1991, ApJ, 374, 202
Davidsen, A. F., et al. 1991, ApJ, in preparation
Fesen, R. A., Blair, W. P., & Kirshner, R. P. 1982, ApJ, 262, 171
Hartigan, P., Raymond, J., & Hartmann, L. 1987, ApJ, 316, 323 (HRH)
Hester, J. J. 1987, ApJ, 314, 187
Hester, J. J., Parker, R. A. R., & Dufour, R. J. 1983, ApJ, 273, 219
Hester, J. J., Raymond, J. C., & Danielson, G. 1986, ApJ, 303, L17
Innes, D. E., Giddings, J. R., & Falle, S. A. E. G. 1987, MNRAS, 226, 67
Jenkins, E. B., Silk, J., & Wallerstein, G. 1976, ApJS, 32, 681
Longo, R., Stalio, R., Polidan, R. S., & Rossi, L. 1988, ApJ, 339, 478
Mathis, J. S. 1990, ARAA, 28, 37
McKee, C. F., & Draine, B. T. 1991, Science, 252, 397
Osterbrock, D. E. 1989, Astrophysics of Gaseous Nebulae and Active Galactic Nuclei (Mill Valley: University Science Books), 81
Rasmussen, A., & Martin, C. 1990, BAAS, 22, 1272
Raymond, J. C., Black, J. H., Dupree, A. K., Hartmann, L., & Wolff, R. S. 1981, ApJ, 246, 100
Raymond, J. C., Blair, W. P., Fesen, R. A., & Gull, T. R. 1983, ApJ, 275, 636
Raymond, J. C., Wallerstein, G., & Balick, B. 1991, ApJ, in press
Shemansky, D. E., Sandel, B. R., & Broadfoot, A. L. 1979, ApJ, 231, 35